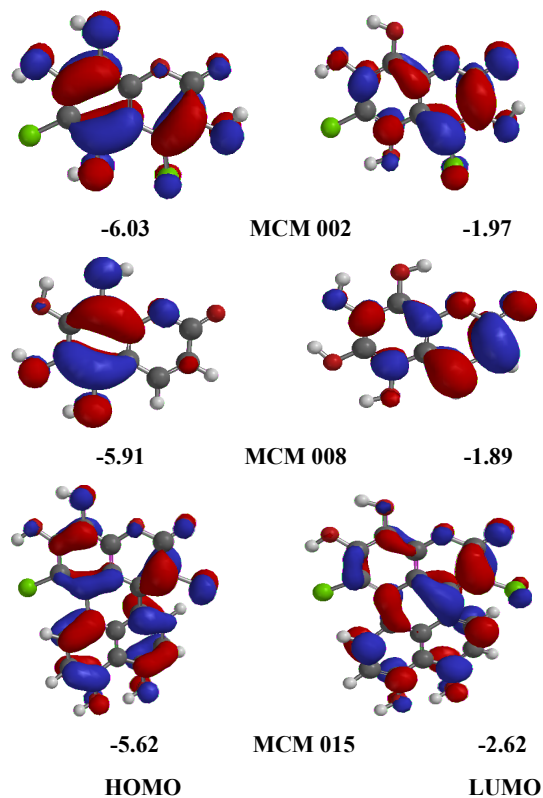


In Silico design of hydroxylated coumarins and thermodynamic investigation of their free radical scavenging mechanism

I.O. Alisi*, A. Uzairu and S.O. Idris



Highlights

- New set of coumarin antioxidants with improved free radical scavenging potency were successfully designed by ligand based virtual screening technique.
- The radical scavenging mechanism of these antioxidants were investigated by thermodynamic studies.
- These compounds could scavenge $\text{HOO}\cdot$ and $\text{CH}_3\text{OO}\cdot$ radicals by HAT, SET-PT and SPLET mechanisms in the gas phase and aqueous solution.
- The present research is a gateway towards the efficient exploitation of these compounds in the field of food chemistry and pharmacy.

RESEARCH ARTICLE

In Silico design of hydroxylated coumarins and thermodynamic investigation of their free radical scavenging mechanism

I.O. Alisi^{1*}, A. Uzairu² and S.O. Idris²

¹Department of Applied Chemistry, Federal University Dutsinma, P.M.B. 5001 Dutsinma, Katsina State, Nigeria.

²Department of Chemistry, Ahmadu Bello University Zaria, P.M.B. 1045 Zaria, Kaduna State, Nigeria.

Received: 23/12/2019; Accepted: 14/09/2020

Abstract: Coumarin and its derivatives have been found to exhibit antioxidant activities. However, a detailed description of the thermodynamics of free radical scavenge by these compounds has not received adequate attention. In order to explore the reaction energetics of the free radical scavenging mechanism of newly designed coumarin compounds, a theoretical study, based on density functional theory (DFT) using the Becke's three-parameter Lee-Yang-Parr hybrid functional (B3LYP) in connection with the 6-311G* basis set, was employed. Hydrogen atom transfer (HAT), single electron transfer followed by proton transfer (SET-PT) and sequential proton loss electron transfer (SPLET) mechanisms were investigated by thermodynamic studies in the gas phase and aqueous solution. Various reaction enthalpies such as bond dissociation enthalpy (BDE), adiabatic ionization potential (AIP), proton dissociation enthalpy (PDE), proton affinity (PA), electron transfer enthalpy (ETE) and Gibbs free energy changes that characterize these mechanisms were calculated. The high solvation enthalpies of the electron and proton resulted in lower values of AIP and PA respectively in aqueous solution than in the gas phase. The reaction Gibbs free energy results indicate that hydroxylated coumarin molecules are efficient free radical scavengers by HAT and SPLET mechanisms in the gas phase and aqueous solution. The SET-PT mechanism was thermodynamically prohibited in the gas phase, but feasible in aqueous solution. Also these compounds were observed to be more reactive towards HOO· than CH₃OO· radicals.

Keywords: Antioxidants; free radicals; coumarins; Gibbs free energy; *In Silico* Design.


INTRODUCTION

The coumarins belong to the benzopyrone family, which are abundantly distributed among the plant genus *Calophyllum*. They occur in the fruits, leaves, stems and roots (Jain Joshi, 2012). They represent a class of active compounds associated with a wide spectrum of important biological activities such as anti-inflammatory (Liu *et al.*, 2018; Arora *et al.*, 2014), antiviral (Shen *et al.*, 2018), antitumor (Liu *et al.*, 2018; Salem *et al.*, 2016; An *et al.*, 2018), antibacterial (Khan *et al.*, 2004), antifungal (Khan *et al.*, 2004; Forezi *et al.*, 2018), anticancer (Morsy *et al.*, 2017) and anticoagulant (Lei *et al.*, 2015) activities. Also, the antioxidant activities of coumarin and its derivatives

have been investigated widely (Liu *et al.*, 2018; Arora *et al.*, 2014; Salem *et al.*, 2016; Pe'rez-Cruz *et al.*, 2018; Onar and Vardar, 2018; Xia *et al.*, 2018). Antioxidants are compounds that scavenge free radicals by employing various mechanisms in their mode of action in the human system. Three major mechanisms of free radical scavenging have been recognised. They include, hydrogen atom transfer (HAT), single electron transfer followed by proton transfer (SET-PT) and sequential proton loss electron transfer (SPLET) (Medina *et al.*, 2014; Ngo *et al.*, 2016; Bayat and Fattahi, 2017). The trend in the implication of oxidative damage in many pathology cases (e.g. atherosclerosis, hypertension, diabetes, and cardiovascular diseases) has triggered interest in the design and synthesis of new antioxidants with potent free radical scavenging properties. However, the mechanism of free radical scavenge by these compounds needs to be analysed.

In this research, the earlier developed quantitative structure activity relationship (QSAR), model for coumarin antioxidants (Alisi *et al.*, 2018), was employed in the design of a new set of coumarin compounds by ligand based virtual screening technique. Virtual screening by the method of QSAR is highly beneficial in the prediction and identification of new biologically active compounds. (Melagraki *et al.*, 2009; Asadollahi *et al.*, 2011). This technique has emerged as a reliable, quick and cost-effective technique for the discovery of lead compounds. The QSAR model was also employed in predicting the antioxidant activities of the designed compounds. The applicability domain of these compounds was accessed by the leverage approach. Three of the compounds with best antioxidant activities were subjected to thermodynamic studies in order to generate the various reaction enthalpies that influence their antioxidant mechanisms. The frontier orbital energies of the molecules and the spin density distribution of their radicals were computed. Three reaction mechanisms namely, HAT, SET-PT and SPLET, were considered. The various reaction enthalpies namely, the electron transfer enthalpy (ETE), the adiabatic ionization potential (AIP), the bond dissociation enthalpy (BDE), the proton dissociation enthalpy (PDE) and the proton affinity (PA), that characterize the various steps in these mechanisms were computed.

*Corresponding Author's Email: ikeogadialisi@gmail.com

 <https://orcid.org/0000-0002-1985-3228>



A crucial factor that influences the radical scavenging mechanism is the characteristics of the free radicals scavenged (Amic' *et al.*, 2017; Xie *et al.*, 2014). The HOO· and CH₃-OO· are examples of peroxy radicals (ROO·), which also includes methyl peroxy radical (CH₃-OO·), vinyl peroxy radical (CH₂=CH-OO·), allyl peroxy radical (CH₂=CH-CH₂-OO·), etc. The ROO· are formed within living systems and have been proposed as free radicals of biological relevance which need to be efficiently scavenged in order to retard oxidative stress (Galano and Alvarez-Idaboy, 2013). This is attributed to their moderate half-lives, which are an efficient requirement for interception by phenolic compounds. They may mimic lipid peroxy radicals (LOO·), which are abundantly formed in biological systems. The thermodynamically preferred mechanism of free radical scavenging in the present research was decided by calculating the Gibbs free energy change of the reaction ($\Delta_r G$), for scavenging the two important peroxy radicals, the hydroperoxyl radical (HOO·) and the methyl peroxy radical (CH₃OO·) in the gas phase and aqueous solution.

MATERIALS AND METHODS

In Silico design of new compounds

With the aid of the developed QSAR model for coumarin antioxidants (Alisi *et al.*, 2018), a new set of coumarin antioxidants were designed by ligand based virtual screening. This was achieved by insertion, deletion and substitution of different substitutes on the template molecule as dictated by the results of the coumarin antioxidant model (Melagraki *et al.*, 2009; Asadollahi *et al.*, 2011; Mitra *et al.*, 2011; Alisi *et al.*, 2019). Compound M45 (Fig. 1) listed in Table 1 of (Alisi *et al.*, 2018), was observed to possess the best antioxidant activity ($pIC_{50} = 5.769$). Based on this reason, it was chosen as the template molecule in the present research.

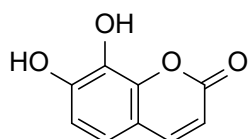


Figure 1: The parent coumarin molecule used as template (M45).

The chemical structures of the compounds were drawn with the aid of the ChemDraw program (Li *et al.*, 2004). Also, minimization and further optimization of the molecular structures were accomplished at the density functional theory (DFT), level using the Becke's three-parameter Lee-Yang-Parr hybrid functional (B3LYP), and 6-311G* basis set without symmetry constraints with the aid of Spartan 14 program (Shao *et al.*, 2006). Through this computation, quantum chemical descriptors were generated. The optimized structures were converted into Sdf files and submitted for the generation of molecular descriptors using the PADEL program package version 2.20 (Yap, 2011). The effects of the structural modifications on the antioxidant activity of the resulting compounds were investigated using the coumarin antioxidant model. Subsequently, the applicability domains of the designed

coumarins were assessed by the leverage approach.

Calculation of antioxidant descriptors

The evaluation of the preferred mechanism of free radical scavenge was accomplished by the computation of various antioxidant descriptors in the gas phase and aqueous solution as presented below:

The homolytic bond dissociation enthalpy (BDE), was calculated under standard conditions of 1 atm. and 298.15 K using Eq. 1. BDE is the standard enthalpy change at a given temperature when a particular chemical bond is broken under standard conditions (Ruscic, 2015). The BDE value determines the stability of the corresponding hydroxyl group. When the BDE value is low, the stability of the corresponding O-H bond is low, and thus can easily be broken (Sun and Jin, 2013). This gives rise to better antioxidant activity for the considered molecule.

$$BDE = H_{\text{radical}} + H_H - H_{\text{neutral}} \quad (1)$$

Adiabatic ionization potential (AIP), values represents the ability of the antioxidant to transfer electrons to the free radical. It describes the process of electron donation by the antioxidant. The lower the AIP value for a given molecule, the easier is the ability to transfer electrons. Molecules with lower AIP values have higher tendency to undergo ionization. Such molecules have been observed to possess stronger antioxidant activities (Işın, 2016). The AIP values were estimated according to Eq. (2);

$$AIP = H_{\text{cation radical}} + H_{\text{electron}} - H_{\text{neutral}} \quad (2)$$

The proton dissociation enthalpy (PDE), describes the ability of the molecules to donate protons. The computation of PDE values was accomplished using Eq. (3). Antioxidants with lower PDE values are more susceptible to proton abstraction (Mikulski *et al.*, 2014).

$$PDE = H_{\text{radical}} + H_{H^+} - H_{\text{cation radical}} \quad (3)$$

Proton affinity (PA) is the molar enthalpy change at 298.15 K. lower PA values result in higher antioxidant activity of molecules. This parameter was calculated using Eq. (4);

$$PA = H_{\text{anion}} + H_{H^+} - H_{\text{neutral}} \quad (4)$$

The electron transfer enthalpy (ETE), values were calculated using Eq. (5). The lower the ETE value for a given molecule, the more active is the resulting phenoxide anion.

$$ETE = H_{\text{radical}} + H_{\text{electron}} - H_{\text{anion}} \quad (5)$$

where,

H_{radical} = Total enthalpy of phenoxyl radical.

H_H = Total enthalpy of the hydrogen atom.

H_{neutral} = Total enthalpy of neutral compound.

H_{H^+} = Total enthalpy of the proton.

$H_{\text{cation radical}}$ = Total enthalpy of the cation radical.

H_{electron} = Total enthalpy of the electron

H_{anion} = Total enthalpy of the anion.

In this study, the total enthalpies of the species were

obtained as the sum of total electronic energy, zero-point energy and the translational, rotational and vibrational contributions to the total enthalpy as presented in Eq. 6. The RT (PV-work) term was added to convert the energy to enthalpy (Najafi *et al.*, 2011).

$$H = E_0 + ZPE + H_{trans} + H_{rot} + H_{vib} + RT \quad (6)$$

Where, are the translational, rotational, and vibrational contributions to the enthalpy respectively.

E_0 is the total energy at 0 K.

ZPE = zero-point vibrational energy.

Also, for the computation of the antioxidant descriptors, the following values were employed; $H(H^*)_{vacuum} = -1312.479673$ kJ/mol, $H(H^*)_{vacuum} = 6.1961805$ kJ/mol, $H(e^-)_{vacuum} = 3.14534924$ kJ/mol, $H(H^*)_{water} = 3.9907603$ kJ/mol, $H(H^+)_{water} = 1090.00266$ KJ/mol, $H(e^-)_{hydr} = 105$ KJ/mol (Nenadis and Tsimidou, 2012; Bartmess. 1994; Bizarro *et al.*, 1999; Rimarcik *et al.*, 2010). Geometry optimization of all molecular structures in the gas phase was performed at the DFT/B3LYP/6-311G* level of theory. Water ($\epsilon=78.39$) is the physiological medium of human living cells. Consequently, the computation of the solvation effect of water on the antioxidant activity was accomplished using the self-consistent reaction field (SCRF) method with a polarized continuum model (PCM) (Li *et al.*, 2018; Bayat and Fattahi, 2017) at the DFT/B3LYP/6-31G* level.

Investigation of the thermodynamically favoured mechanism

The reaction Gibbs free energy ($\Delta_r G$), is employed to determine the thermodynamically favoured mechanism (Amic' *et al.*, 2017; Zheng *et al.*, 2017). In this research, the changes in Gibbs free energy between the reactants and products in the gas phase and aqueous solution for the studied mechanisms of the reactions between the antioxidants and the peroxy radicals (HOO· and CH₃-OO·) were estimated.

The reaction between a free radical and an antioxidant is said to be thermodynamically favourable if the reaction Gibbs free energy is exergonic (Eq. 7).

$$\Delta_r G = [G(products) - G(reactants)] < 0 \quad (7)$$

The Gibbs free energy change for the HAT mechanism is given by (Eq. 8).

$$\Delta_r G_{BDE} = [G(H_{n-1}Antiox^*) + G(RH)] - [G(H_nAntiox) + G(R^*)] \quad (8)$$

The Gibbs free energy change for the SET-PT mechanism is given by (Eq. 9) and (Eq. 10). While that of the SPLET mechanism is given by (Eq. 11) and (Eq. 12).

$$\Delta_r G_{AIP} = [G(H_{n-1}Antiox^{*+}) + G(R^-)] - [G(H_nAntiox) + G(R^*)] \quad (9)$$

$$\Delta_r G_{PDE} = [G(H_{n-1}Antiox^*) + G(RH)] - [G(H_{n-1}Antiox^{*+}) + G(R^-)] \quad (10)$$

$$\Delta_r G_{PA} = [G(H_{n-1}Antiox^-) + G(RH)] - [G(H_nAntiox) + G(R^-)] \quad (11)$$

$$\Delta_r G_{ETE} = [G(H_{n-1}Antiox^*) + G(R^-)] - [G(H_{n-1}Antiox^-) + G(R^*)] \quad (12)$$

Where,

$G(H_nAntiox)$ = Gibbs free energy of neutral antioxidant.

$G(H_{n-1}Antiox^*)$ = Gibbs free energy of phenoxyl radical.

$G(R^*)$ = Gibbs free energy of free radical.

$G(HR)$ = Gibbs free energy of product formed by hydrogen abstraction to free radical.

$G(H_{n-1}Antiox^{*+})$ = Gibbs free energy of cation radical.

$G(H^+)$ = Gibbs free energy of proton.

$G(R^-)$ = Gibbs free energy of free radical anion.

$G(H_{n-1}Antiox^-)$ = Gibbs free energy of anion.

In the above computations, the values of and were employed as the Gibbs free energy of the electron (e^-) and proton (H^+) respectively in the gas phase. However, in aqueous solution, and were used as the Gibbs free energy for the electron and proton respectively (Tissandier *et al.*, 1998; Hwang and Chung, 2005).

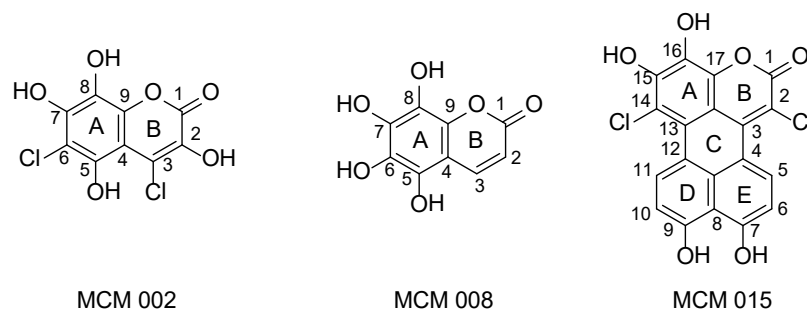
RESULTS AND DISCUSSIONS

Analysis of ligand based virtual screening

A total of twenty coumarin antioxidant derivatives with improved antioxidant activities were successfully designed from the template molecule (Figure 1) and their pIC_{50} results and leverage values calculated and presented in Table 1. All the designed molecules recorded improved antioxidant activity when compared with the template molecule (MCM 45). Also the results of applicability domain investigation for the developed coumarin model gave a leverage threshold, h^* value of 0.4286 (Alisi *et al.*, 2018).

Table 1: Designed coumarin antioxidants, their predicted antioxidant activities and leverage values.

Comp No	Compound Name		Leverage
MCM 01	4,6-difluoro-3,5,7,8-tetrahydroxy-2H-chromen-2-one	12.791	0.500
MCM 02	4,6-dichloro-3,5,7,8-tetrahydroxy-2H-chromen-2-one	12.177	0.302
MCM 03	3,5,7,8-tetrahydroxy-2H-chromen-2-one	11.089	0.145
MCM 04	5,7,8-trihydroxy-2H-chromen-2-one	8.833	0.137
MCM 05	3,7,8-trihydroxy-2H-chromen-2-one	7.958	0.111
MCM 06	4,7,8-trihydroxy-2H-chromen-2-one	8.381	0.083
MCM 07	6,7,8-trihydroxy-2H-chromen-2-one	8.632	0.267
MCM 08	5,6,7,8-tetrahydroxy-2H-chromen-2-one	11.529	0.334
MCM 09	7,8-dihydroxy-5-(4-hydroxyphenyl)-2H-chromen-2-one	7.581	0.250
MCM 10	7,8-dihydroxy-4-(4-hydroxyphenyl)-2H-chromen-2-one	7.633	0.260
MCM 11	3-chloro-7,8-dihydroxy-5-(4-hydroxyphenyl)-2H-chromen-2-one	9.275	0.133
MCM 12	6-chloro-7,8-dihydroxy-4-(4-hydroxyphenyl)-2H-chromen-2-one	9.160	0.135
MCM 13	3,6-dichloro-7,8-dihydroxy-5-(4-hydroxyphenyl)-2H-chromen-2-one	9.833	0.171
MCM 14	3,6-dichloro-7,8-dihydroxy-4-(4-hydroxyphenyl)-2H-chromen-2-one	9.882	0.181
MCM 15	1,6-dichloro-4,5,9,10-tetrahydroxy-2H-phenalenol[1,2,3-de]chromen-2-one	12.898	0.376
MCM 16	6,7,8-trihydroxy-5-(4-hydroxyphenyl)-2H-chromen-2-one	11.075	0.194
MCM 17	7,8-dihydroxy-4-(4-hydroxyphenyl)-2H-chromen-2-one	8.616	0.152
MCM 18	1,4,5,6,9,10-hexahydroxy-2H-phenalenol[1,2,3-de]chromen-2-one	15.109	0.776
MCM 19	4-chloro-7,8-dihydroxy-2-oxo-2H-chromene-5-carboxylic acid	7.953	0.239
MCM 20	5-chloro-7,8-dihydroxy-2-oxo-2H-chromene-4-carboxylic acid	8.031	0.256

**Figure 2:** Chemical structures and carbon atom numbering of MCM 002, MCM 008 and MCM 015 molecules.

The calculated leverage results for the coumarin molecules revealed the presence of two structural outliers, which are outside the applicability domain of the developed coumarin antioxidant model. These include MCM 001 and MCM 018 molecules. The remaining molecules were found within the applicability domain of the coumarin model with MCM 002, MCM 008, and MCM 015 having the best antioxidant activities. The molecular structures of these compounds are presented in Figure 2.

It was observed that the molecule MCM 015, which has the best antioxidant activity among the designed molecules, contains two phenol groups which are hydrogen donor groups attached at positions 3 and 13, and two chlorine atoms which are electronegative groups attached at positions 2 and 14 on rings B and A, respectively. The two phenol groups are fused together to give a total of five rings for this molecule. This unique structure gave rise to the exceptionally good antioxidant activity of this molecule as reflected in its pIC_{50} value (Table 1).

Analysis of the HAT mechanism

The calculated BDE results at the various OH positions for MCM 002, MCM 008 and MCM 015 in the gas phase and aqueous solution are presented in Table 2. For MCM 002, the BDE at the 2-OH position in vacuum has the highest value of 317.72 kJ/mol in comparison to the other positions which have values of 276.11 kJ/mol, 287.37 kJ/mol and 274.08 kJ/mol at the 5-OH, 7-OH and 8-OH positions respectively. The high BDE value of MCM 002 at the 2-OH position could be attributed to the existence of an intramolecular hydrogen bond between the 2-OH and the adjacent ketone group in the parent molecule. Observe that hydrogen abstraction from 2-OH also requires breaking the intramolecular hydrogen bond. The existence of a hydrogen bond also accounts for the high BDE of MCM 008 at the 8-OH position and MCM 015 at the 16-OH position.

The lowest BDE for MCM 002 occurred at the 8-OH with a value of 274.08 kJ/mol (Table 2). This is closely followed by that at the 5-OH position with a value of 276.11

Table 2: Antioxidant descriptors of designed coumarin antioxidants calculated at the DFT/B3LYP/6-311G*/6-31G* levels in vacuum and aqueous solution.

Comp No	HAT		SET-PT				SPLET				Radical Spin Density
	BDE (kJ/mol)		AIP (kJ/mol)		PDE (kJ/mol)		PA (kJ/mol)		ETE (kJ/mol)		
	Gas	Water	Gas	Water	Gas	Water	Gas	Water	Gas	Water	
MCM 002 2-OH	317.72	274.47	447.43	404.08	1192.11	-1320.63	1341.50	90.48	298.04	-1007.02	2.28×10 ⁻⁴
MCM 002 5-OH	276.11	207.15	557.84	387.99	1040.09	-1371.85	1359.51	104.21	238.42	-1088.07	1.78×10 ⁻⁴
MCM 002 7-OH	287.37	277.80	579.81	393.29	1029.38	-1306.50	1309.47	74.748	299.72	-987.96	2.16×10 ⁻⁴
MCM 002 8-OH	274.08	198.78	571.86	379.12	1024.05	-1371.35	1337.48	93.84	258.42	-1086.07	1.59×10 ⁻⁴
MCM 008 5-OH	282.63	280.61	584.10	351.15	1020.35	-1261.55	1368.12	109.55	236.33	-1019.95	2.08×10 ⁻⁴
MCM 008 6-OH	280.57	276.89	584.44	411.03	1017.95	-1325.15	1362.97	109.58	239.42	-1023.70	2.05×10 ⁻⁴
MCM 008 7-OH	288.94	282.97	588.86	444.85	1021.90	-1352.90	1342.10	91.44	268.67	-999.49	2.11×10 ⁻⁴
MCM 008 8-OH	289.97	289.06	581.61	407.99	1030.18	-1309.94	1391.63	86.42	220.16	-988.37	2.69×10 ⁻⁴
MCM 015 7-OH	257.86	225.16	540.90	375.75	1038.78	-1341.6	1261.16	125.37	318.52	-1091.22	0.69×10 ⁻⁴
MCM 015 9-OH	253.79	222.62	539.09	379.96	1036.52	-1348.35	1265.62	127.26	309.99	-1095.65	0.63×10 ⁻⁴
MCM 015 15-OH	292.88	268.46	556.63	376.86	1058.08	-1299.41	1331.58	117.91	283.13	-1040.47	2.08×10 ⁻⁴
MCM 015 16-OH	312.23	275.47	546.55	367.77	1087.51	-1283.32	1325.48	89.03	308.57	-1004.58	2.47×10 ⁻⁴
Phenol	327.55	293.71	572.78	180.52	1076.59	-1077.82	1462.89	141.47	186.48	-1038.75	

kJ/mol. These results confirm that HAT from the 8-OH or 5-OH occurs more readily than from the 7-OH or 2-OH positions. Therefore, the primary site of free radical attack on the MCM 002 molecule, based on the HAT mechanism, has almost equal chances at either the 8-OH or 5-OH positions. Similarly, MCM 015 with lowest values of BDE at the 9-OH (253.79 kJ/mol) position, has this position as the most probable site for free radical attack based on the HAT mechanism. For MCM 008, four possible sites for HAT exist with their associated BDE's namely; the 5-OH (282.63 kJ/mol), 6-OH (280.57 kJ/mol), 7-OH (288.94 kJ/mol) and 8-OH (289.97 kJ/mol). These positions have very close BDE with the 6-OH having the lowest value, while the 8-OH has the highest value. This implies that there are very close chances of HAT occurring in any of the four -OH positions with the 6-OH position having the greatest chance. A similar sequence with lower BDE values was observed in aqueous solution. The results of BDE for the three compounds at all the possible sites of free radical attack are lower than that of phenol (327.55 kJ/mol) which is usually considered as a reference compound. This shows that these compounds are better free radical scavengers than phenol through HAT. From the results presented in Table 2, the BDE values in water are lower than the corresponding values in gas. For instance, the BDE value of MCM 015 at the 9-OH site in vacuum is 253.79 kJ/mol. While the value in water is 222.62 kJ/mol. This suggests that HAT mechanism is more preferred in aqueous solution than in the gas phase.

Analysis of spin density distribution

To explain the differences in the BDE results, the spin density distribution of MCM 002, MCM 008 and MCM 015 radicals were calculated and presented in Table 2. The spin density distribution is a useful parameter employed in rationalising the stability of the antioxidant radical (Xue *et al.*, 2014; Wang *et al.*, 2015; Zheng *et al.*, 2017). The lower

the spin density on the radical, the more delocalised is the spin density, the easier the radical is formed, the higher the stability of the radical, the lower the BDE, the higher the antioxidant activity of the compound. As presented in Table 2, results of the spin density on the oxygen atom of these different OH radicals indicate that the stabilization of these radicals for MCM 002 increases in the order MCM 002 2-OH < MCM 002 7-OH < MCM 002 5-OH < MCM 002 8-OH. Similarly for MCM 008 radicals, we have MCM 008 8-OH < MCM 008 7-OH < MCM 008 5-OH < MCM 008 6-OH. Also, the increasing order for MCM 015 radicals is: MCM 015 16-OH < MCM 015 15-OH < MCM 015 7-OH < MCM 015 9-OH. This is in very good agreement with the order in which their BDE decrease. Further, the density is more delocalised for radicals issued from MCM 002 8-OH, MCM 008 6-OH and MCM 015 9-OH for the three considered antioxidant compounds respectively. These are the sites with the lowest BDE value, and subsequently the preferred site of free radical scavenge in each of these molecules.

Analysis of SET-PT mechanism

The results of adiabatic ionization potential (AIP) and proton dissociation enthalpy (PDE) for the studied molecules and their radicals in vacuum and water are presented in Table 2. The first step of the SET-PT mechanism is characterized by AIP. Among the various sites that are subject to electron abstraction for the MCM 002 molecule in vacuum, the 2-OH site is observed to possess the highest electron donation ability to the free radical, since it has the lowest AIP value of 447.43 KJ/mol. This value is also lower than that of phenol (572.78 kJ/mol) computed at the same level of theory. This implies that electron abstraction at this site is more favoured than that of phenol. The MCM 008 molecule has very close results for the various sites with the 8-OH position having the lowest value of 581.61 kJ/mol. The results of AIP for

all the sites in this molecule are higher than that of phenol (Table 2). This indicates that this molecule has a less tendency to donate electrons as compared to phenol. The AIP results for MCM 015 lie within the range 539.09 kJ/mol (MCM 015 9-OH) to 556.63 kJ/mol (MCM 015 15-OH). These results show that MCM 015 at the various possible sites possess stronger electron donating ability than phenol with the 9-OH sites having the best potential. In aqueous solution, the AIP results are by far lower than the corresponding values in vacuum. Consequently, these molecules possess higher tendency to lose electrons to the free radical in aqueous solution than in vacuum. The lower AIP values in aqueous solution could be attributed to the high solvation enthalpies of the electron.

The PDE characterizes the second step of the SET-PT mechanism. The general trend of PDE is analogous to that of BDE (Table 2). This is due to the fact that proton dissociation results in radical formation as in bond dissociation. The molecules of MCM 002, MCM 008 and MCM 015 have lowest PDE values of 1024.05 kJ/mol, 1017.95 kJ/mol and 1036.52 kJ/mol at the 8-OH, 6-OH and 9-OH positions respectively in vacuum. These values are lower than that of the reference molecule (phenol) which has a value of 1076.59 kJ/mol at the same computation level. This suggests that these molecules at the stated sites possess greater proton dissociation ability than phenol. Also, the observed results of PDE in water are lower than the corresponding values in vacuum. For reactions that involve multiple step mechanism such as the SET-PT, the first step is the most important from a thermodynamic view point. Therefore the results of AIP dominate those of PDE.

Analysis of SPLET mechanism

The proton affinity (PA) and electron transfer enthalpy (ETE) results for MCM 002, MCM 008 and MCM 015 in vacuum and water are presented in Table 2. The antioxidant parameter employed in the quantification of the first step of a SPLET mechanism is PA, whereas, the second step is quantified by ETE. For each of the title molecules, MCM 002, MCM 008 and MCM 015, the highest recorded PA results in vacuum occurred at the 5-OH, 8-OH and 15-OH positions with values of 1359.51 kJ/mol, 1391.63 kJ/mol and 1331.58 kJ/mol respectively. This demonstrates that the formation of phenoxide anion at these positions is more difficult than at other positions for each of the considered molecules. This could be attributed to the formation of an intramolecular hydrogen bond between the OH groups at these positions and the respective electronegative groups such as chlorine or oxygen. The lowest results of PA in vacuum for each of the molecules MCM 002, MCM 008 and MCM 015 occurred at the 7-OH site with values of 1309.47 kJ/mol, 1342.10 kJ/mol and 1261.16 kJ/mol respectively. These are the preferred sites for deprotonation in each of the molecules. The PA values in water are by far lower than the corresponding values in vacuum. This is a consequence of the high solvation enthalpy of the proton. Also, the computed results of PA at all the considered sites for each of the molecules MCM 002, MCM 008 and MCM 015 in both vacuum and water are lower than the corresponding values for phenol (1462.89 kJ/mol in vacuum; 141.47 in

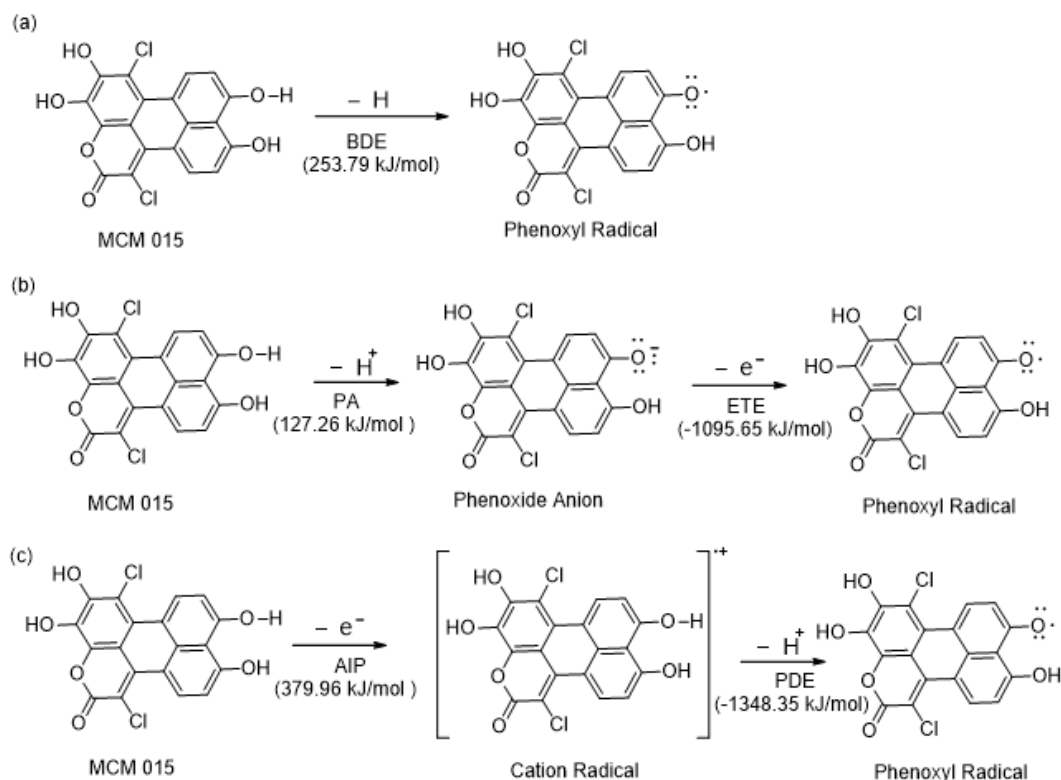
water).

For the molecule MCM 002, the lowest ETE value of 238.42 kJ/mol was observed at the 5-OH position in vacuum. In MCM 008, this was observed at the 8-OH position with ETE values of 220.16 kJ/mol and -988.37 kJ/mol in vacuum and water respectively. For MCM 015 molecule, the lowest ETE value was also observed in ring A in both media. The 5-OH and 8-OH positions are located on ring A of the coumarin moiety. This result indicates that the OH group in ring A contributes greatly to the second step of the SPLET mechanism compared to other rings of coumarin antioxidants. Observe that the ETE value in each case is lower in water than in air. This trend cuts across all the considered sites for the three molecules. From Table 2, the observed results of ETE for each of the molecules in vacuum are lower than those of AIP. Consequently, the single electron transfer from the anionic form of the coumarin antioxidant to the free radical is preferred to that from the neutral form. This is in line with literature results (Rimarcik *et al.*, 2010; Xue *et al.*, 2014; Wang *et al.*, 2015).

Thermodynamically preferred mechanism

The Gibbs free energy changes of reactions of inactivation of $\text{HOO}\cdot$ and $\text{CH}_3\text{OO}\cdot$ by coumarin antioxidant molecules via the HAT, SET-PT and SPLET mechanisms in vacuum and water are reported in Tables 3 and 4 respectively. Results that emanate from the $\Delta_r G$ computation are useful parameters employed in the assignment of the free radical scavenging potency of molecules, because more negative values of the reaction Gibbs free energy change ($\Delta_r G$) represent the thermodynamically more preferred reactions. The molecules of MCM 002, MCM 008 and MCM 015 are able to effectively scavenge $\text{HOO}\cdot$ and $\text{CH}_3\text{OO}\cdot$ by HAT and SPLET mechanisms in vacuum and water at all their considered sites of free radical scavenge, because these processes are exergonic. In both the gas phase and aqueous solution, the exergonicity of $\Delta_r G_{PA}$ in the first step overwhelmed the endergonicity of $\Delta_r G_{ETE}$ in the second step of the SPLET mechanism, since a thermodynamically unfavourable reaction could be driven by thermodynamically favourable reaction that is coupled to it. These molecules are not able to scavenge $\text{HOO}\cdot$ and $\text{CH}_3\text{OO}\cdot$ by SET-PT mechanism in vacuum, because the first step ($\Delta_r G_{AIP}$) which is the most important is endergonic, while the second step ($\Delta_r G_{PDE}$) is exergonic. Consequently, the entire SET-PT pathway is not feasible in vacuum. In aqueous solution, the first step ($\Delta_r G_{AIP}$) is exergonic and overwhelmed the endergonicity of the second step ($\Delta_r G_{PDE}$). Subsequently, the entire process is exergonic and thermodynamically feasible in aqueous solution.

A comparison of the results presented in Tables 3 and 4, reveals that the investigated coumarin antioxidants are better free radical scavengers for $\text{HOO}\cdot$ than $\text{CH}_3\text{OO}\cdot$ radicals by HAT, SPLET and SET-PT mechanisms. Among the tested molecules, MCM 015 at the 9-OH position exhibited the highest level of exergonicity in its reactions based on the computed results of $\Delta_r G$. Consequently, the reactions of inactivation of free radicals by MCM 015 via HAT, SPLET and SET-PT mechanisms are presented in Scheme 1 (a), (b) and (c) respectively.



Scheme 1: (a) HAT mechanism of MCM 015 in vacuum (b) SPLET mechanism of MCM 015 in water (c) SET-PT mechanism of 015 in water.

Table 3: Gibbs free energy changes (in kJ/mol) of scavenging HOO. by coumarin antioxidants at the DFT/B3LYP/6-311G*/6-31G* levels in vacuum and aqueous solution.

Comp No	HAT		SET-PT				SPLET			
	$\Delta_r G_{BDE}$		$\Delta_r G_{AIP}$		$\Delta_r G_{PDE}$		$\Delta_r G_{PA}$		$\Delta_r G_{ETE}$	
	Gas	Water	Gas	Water	Gas	Water	Gas	Water	Gas	Water
MCM 002 2-OH	-3.72	-40.59	577.77	-209.86	-581.49	169.27	-293.37	-103.10	289.65	62.51
MCM 002 5-OH	-32.79	-45.73	688.44	-239.00	-721.22	193.27	-135.68	-90.913	102.90	45.18
MCM 002 7-OH	-42.92	-63.72	708.81	-254.94	-751.73	191.22	-324.40	-117.93	281.48	54.21
MCM 002 8-OH	-44.89	-66.71	701.25	-260.27	-746.14	193.56	-296.42	-98.658	251.53	31.95
MCM 008 5-OH	-36.98	-53.26	713.93	-232.66	-750.91	179.41	-266.38	-83.168	229.40	29.91
MCM 008 6-OH	-38.71	-63.99	713.13	-246.40	-751.84	182.41	-270.16	-82.404	231.45	18.42
MCM 008 7-OH	-30.56	-51.83	716.67	-229.12	-747.23	177.29	-291.21	-100.53	260.65	48.70
MCM 008 8-OH	-29.39	-51.24	710.27	-228.49	-739.66	177.25	-243.13	-113.95	213.74	62.71
MCM 015 7-OH	-62.35	-80.29	671.55	-281.93	-733.90	201.65	-373.37	-116.49	311.02	36.20
MCM 015 9-OH	-66.29	-83.44	669.01	-285.34	-735.30	201.91	-368.88	-111.37	302.59	27.93
MCM 015 15-OH	-27.14	-52.38	685.68	-279.38	-712.82	227.01	-303.16	-120.92	276.02	68.55
MCM 015 16-OH	-8.16	-43.16	676.31	-275.39	-684.47	232.23	-309.52	-123.78	301.36	80.62

Analysis of frontier molecular orbitals

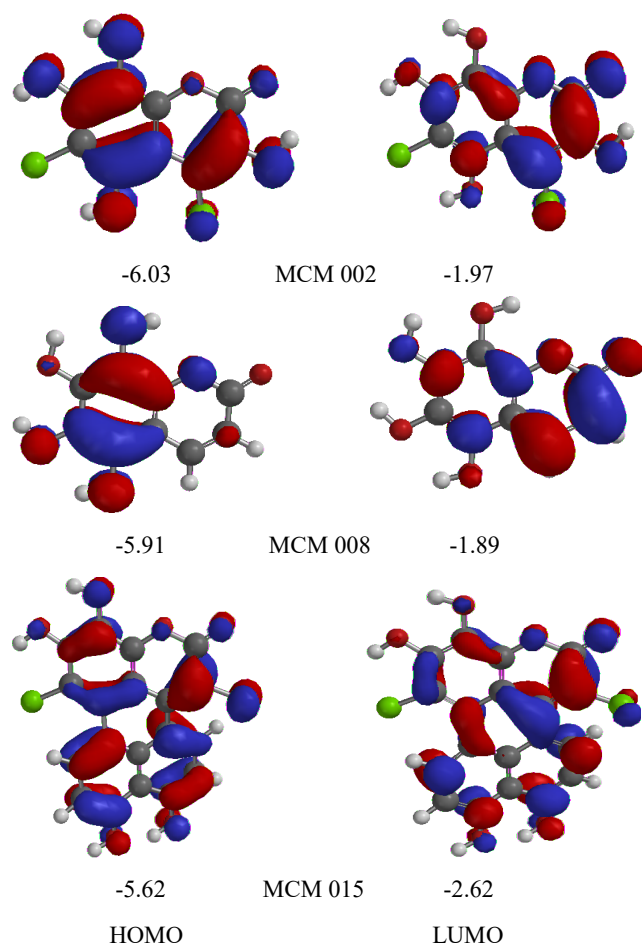
The frontier orbital distributions and energy for MCM 002, MCM 008 and MCM 015 computed at the B3LYP/6-311G* level in the gas phase are presented in Figure 4. The LUMO distribution occurs almost over the entire molecules of MCM 002, MCM 008 and MCM 015. The HOMO appears to be delocalised over the entire molecule of MCM 015. For MCM 008, it is localised on the conjugated carbons of ring A and its associated oxygen atoms. For MCM 002, it

is localised on the oxygen atoms of the hydroxyl group and the conjugated carbons of rings A and B.

From Figure 4, MCM 015 has the highest HOMO energy (-5.62 eV), followed by MCM 008 (-5.91 eV) and MCM 002 (-6.03 eV) with almost equal results. Since molecules with higher HOMO values have stronger electron donating potentials (Xue *et al.*, 2014; Wang *et al.*, 2015; Szeląg *et al.*, 2011; Işın, 2016), MCM 015 will have a higher tendency to donate electrons. Also, the electron donating ability of these molecules predicted by

Table 4: Gibbs free energy changes ($\Delta_r G$ in kJ/mol) of scavenging $\text{CH}_3\text{OO}\cdot$ radical by coumarin antioxidants at the DFT/B3LYP/6-311G*/6-311G* levels in vacuum and aqueous solution.

Comp No	HAT		SET-PT				SPLET			
	$\Delta_r G_{BDE}$		$\Delta_r G_{AIP}$		$\Delta_r G_{PDE}$		$\Delta_r G_{PA}$		$\Delta_r G_{ETE}$	
	Gas	Water	Gas	Water	Gas	Water	Gas	Water	Gas	Water
MCM 002 2-OH	-0.49	-37.96	539.75	-208.41	-540.23	170.45	-252.11	-101.92	251.63	63.96
MCM 002 5-OH	-29.55	-43.11	650.41	-237.55	-679.96	194.44	-94.42	-89.74	64.87	46.63
MCM 002 7-OH	-39.68	-61.09	670.79	-253.49	-710.47	192.40	-283.14	-116.76	243.46	55.67
MCM 002 8-OH	-41.65	-64.08	663.23	-258.82	-704.88	194.73	-255.16	-97.485	213.50	33.4
MCM 008 5-OH	-33.74	-50.63	675.90	-231.21	-709.65	180.58	-225.12	-81.99	191.37	31.37
MCM 008 6-OH	-35.47	-61.36	675.11	-244.94	-710.58	183.58	-228.90	-81.23	193.43	19.87
MCM 008 7-OH	-27.33	-49.20	678.64	-227.66	-705.97	178.46	-249.95	-99.357	222.63	50.15
MCM 008 8-OH	-26.153	-48.61	672.25	-227.03	-698.40	178.42	-201.87	-112.78	175.72	64.16
MCM 015 7-OH	-59.113	-77.66	633.53	-280.48	-692.64	202.82	-332.11	-115.31	273.00	37.65
MCM 015 9-OH	-63.051	-80.81	630.98	-283.89	-694.04	203.08	-327.62	-110.19	264.57	29.39
MCM 015 15-OH	-23.905	-49.75	647.66	-277.93	-671.56	228.18	-261.90	-119.75	238.00	70.00
MCM 015 16-OH	-4.9227	-40.53	638.28	-273.94	-643.21	233.41	-268.26	-122.61	263.34	82.08

**Figure 3:** Orbital distribution and energy (in eV) of HOMO and LUMO for MCM 002, MCM 008 and MCM 015 computed at the B3LYP/6-311G* level in the gas phase.

their HOMO energies follow the same sequence as that of their AIP and BDE at their preferred positions of radical scavenge (Table 2). Consequently, MCM 015 is predicted to have a higher antioxidant activity in comparison to the other two molecules.

CONCLUSION

In the present study, rational design of coumarin antioxidants with improved free radical scavenging properties has been effected by virtual screen using the proposed coumarin antioxidant model. With the aid of the developed model, the molecular structure and antioxidant activities of these molecules were successfully predicted. Among these molecules, MCMM 015 (1,6-dichloro-4,5,9,10-tetrahydroxy-2H-phenalenol[1,2,3-de]chromen-2-one) possessed the best antioxidant activity with a value of 12.898. Our results indicate that the employed screening method is time and cost effective in the design and activity determination of new set of antioxidants.

Three of the best designed molecules namely, MCMM 02, MCMM 08 and MCMM 15 were further subjected to thermodynamic studies by the DFT method in the gas phase and aqueous solution. Reaction enthalpies such BDE, AIP, PDE, PA and ETE which characterise various reaction mechanisms such HAT, SET-PT and SPLET were calculated. In order to rationalise the differences in the BDE values for each molecule, the spin density distributions of the radicals were calculated. All considered coumarin molecules have better hydrogen atom donation ability compared to the reference molecule with MCMM 15 having the best ability as judged from the BDE values. In the gas phase, MCMM 002 at the 2-OH site possessed the strongest electron donation ability from the computed results of AIP. Also from the computed results of PA, the preferred site for deprotonation is the 7-OH position in each of the molecules MCMM 002, MCMM 008 and MCMM 015.

In order to investigate the preferred mechanism of free radical scavenge by each of the antioxidant molecules, the reaction Gibbs free energy change for scavenging $\text{HOO}\cdot$ and $\text{CH}_3\text{OO}\cdot$ at the various OH sites were computed. From the exergonicity of the observed results, the HAT and SPLET mechanisms were thermodynamically feasible in the gas phase and aqueous solution. The SET-PT mechanism was thermodynamically prohibited in the gas phase, but favourable in aqueous solution. Also, the investigated coumarin antioxidants were better scavengers for $\text{HOO}\cdot$ than $\text{CH}_3\text{OO}\cdot$ by these mechanisms. The present study is a gateway to new perspectives towards a rational exploitation of the coumarins in the field of pharmacy and food chemistry.

ACKNOWLEDGEMENT

The authors are grateful to the members of physical chemistry unit in Ahmadu Bello University Zaria, and ICT unit of Federal University Dutsinma for their assistance.

DECLARATION OF CONFLICT OF INTEREST

The authors declare no competing interests.

REFERENCES

- Alisi, I.O., Uzairu, A., Abechi, S.E. and Idris, S.O. (2018). Quantitative Structure Activity Relationship Analysis of Coumarins as Free Radical Scavengers by Genetic Function Algorithm. *Physical Chemistry Research* **6**(1): 208-222. <https://doi.org/10.22036/pcr.2017.95755.1409>.
- Alisi, I.O., Uzairu, A., and Abechi, S.E., (2019). In silico design of hydrazone antioxidants and analysis of their free radical-scavenging mechanism by thermodynamic studies. *Beni-Suef University Journal of Basic and Applied Sciences*, **8**(11): 1-11, <https://doi.org/10.1186/s43088-019-0011-2>.
- Amic', A., Bono, L., Višnja, S., Zoran, M., Svetlana, M., Jasmina, M.D.M. and Dragan, A. (2017). Free radical scavenging potency of quercetin catecholic colonic metabolites: Thermodynamics of $2\text{H}^+/2\text{e}^-$ processes. *Food Chemistry* **218**: 144-151. <https://doi.org/10.1016/j.foochem.2016.09.018>.
- An, R., Hou, Z., Li, J.T., Yu, H.N., Mou, Y.H. and Guo, C. (2018). Design, synthesis and biological evaluation of novel 4-substituted coumarin derivatives as antitumor agents. *Molecules* **23**(9): 2281-2293. <https://doi.org/10.3390/molecules23092281>.
- Arora, R.K., Kaur, N., Bansal, Y. and Bansal, G. (2014). Novel coumarin-benzimidazole derivatives as antioxidants and safer anti-inflammatory agents. *Acta Pharmaceutica Sinica B* **4**(5): 368-375. <https://doi.org/10.1016/j.apsb.2014.07.001>
- Asadollahi, T., Dadfarnia, S., Shabani, A.M.H., Ghasemi, J.B. and Sarkhosh, M. (2011). QSAR models for CXCR2 receptor antagonists based on the genetic algorithm for data preprocessing prior to application of the PLS linear regression method and design of the new compounds using *in silico* virtual screening. *Molecules*, **16**(3): 1928-1955. <https://doi.org/10.3390/molecules16031928>
- Bartmess, J.E. (1994). Thermodynamics of the electron and the proton. *Journal of Physical Chemistry* **98**(25): 6420-6424. <https://doi.org/10.1021/j100076a029>
- Bayat, A. and Fattahi, A. (2017). The free radical scavenging activity of Lespedezacoumestan toward $\cdot\text{OH}$ radical: A quantum chemical and computational kinetics study. *Journal of Physical Organic Chemistry* e3755. <https://doi.org/10.1002/poc.3755>.
- Bizarro, M.M., Cabral, B.J.C., Santos, R.M.B. and Simoes, J.A.M. (1999). Substituent effects on the O-H bond dissociation enthalpies in phenolic compounds: Agreements and Controversies. *Pure and Applied Chemistry* **71**(7): 1249-1256. <https://doi.org/10.1351/pac199971071249>
- Forezi, L.S.M., Borba-Santos, L.P., Cardoso, M.F.C., Ferreira, V.F., Rozental, S. and Silva, C.F. (2018). Synthesis and antifungal activity of coumarins derivatives against *Sporothrix* spp. *Current Topics in Medicinal Chemistry* **18**(2): 164-171. <https://doi.org/10.2174/1568026618666180221115508>
- Galano, A. and Alvarez-Idaboy, J.R. (2013). A Computational Methodology for Accurate Predictions of Rate Constants in Solution: Application to the

- Assessment of Primary Antioxidant Activity. *Journal of Computational Chemistry*, **34**(28): 2430-2445. <https://doi.org/10.1002/jcc.23409>.
- Hwang, S. and Chung, D.S. (2005). Calculation of the solvation free energy of the proton in methanol. *Bulletin of the Korean Chemical Society* **26**(4): 589-593. <https://doi.org/10.5012/bkcs.2005.26.4.589>.
- İşın, O.D. (2016). Theoretical study on the investigation of antioxidant properties of some hydroxyanthraquinones. *Molecular Physics* **114**(24): 3578-3588. <https://doi.org/10.1080/00268976.2016.1248514>.
- Jain, P. K. and Joshi, H. (2012). Coumarin: Chemical and pharmacological profile. *Journal of Applied Pharmaceutical Science* **2** (6): 236-240. <https://doi.org/10.7324/JAPS.2012.2643>.
- Khan, K.M., Saify, Z.S., Khan, M.Z., Ullah, Z., Choudhary, M.I., Rahman, A., Perveen, S., Chohan, Z.H. and Supuran, C.T. (2004). Synthesis of Coumarin Derivatives with Cytotoxic, Antibacterial and Antifungal Activity. *Journal of Enzyme Inhibition and Medicinal Chemistry* **19**(4): 373-379. <https://doi.org/10.1080/14756360409162453>.
- Lei, L., Xue, Y.B., Liu, Z., Peng, S.S., He, Y., Zhang, Y., Fang, R., Wang, J.P., Luo, Z.W., Yao, G.M., Zhang, J.W., Zhang, G., Song, H.P. and Zhang, Y.H. (2015). Coumarin Derivatives from *Ainsliaea Fragrans* and their Anticoagulant Activity. *Scientific Reports* **5**: 13544-13553. <https://doi.org/10.1038/srep13544>.
- Li, Z., Wan, H., Shi, Y. and Ouyang, P. (2004). Personal experience with four kinds of chemical structure drawing software: Review on Chemdraw, Chemwindow, ISIS/Draw, and Chems sketch. *Journal of Chemical Information and Computer Sciences* **44**(5): 1886-1890. <https://doi.org/10.1021/ci049794h>.
- Li, Y., Toscano, M., Mazzone, G., Russo, N. (2018). Antioxidant properties and free radical scavenging mechanisms of cyclocurcumin, *New Journal of Chemistry* **42**(15): 2698-12705. <https://doi.org/10.1039/c8nj01819g>.
- Liu, Y.T., Gong, P.H., Xiao, F.Q., Shao, S., Zhao, D.Q., Yan, M.M. and Yang, X.W. (2018). Chemical constituents and antioxidant, anti-inflammatory and anti-tumor activities of *Melilotus officinalis* (Linn.) Pall. *Molecules* **23**(2): 271-283. <https://doi.org/10.3390/molecules23020271>.
- Medina, M.E., Iuga, C. and Alvarez-Idaboy, J.R. (2013). Antioxidant activity of propyl gallate in aqueous and lipid media: A theoretical study. *Physical Chemistry Chemical Physics* **15**(31): 13137-13146. <https://doi.org/10.1039/C3CP51644J>.
- Melagraki, G., Afantitis, A., Sarimveis, H., Koutentis, P.A., Kollias, G. and Igglessi-Markopoulou, O. (2009). Predictive QSAR workflow for the in silico identification and screening of novel HDAC inhibitors. *Molecular Diversity*, **13**(3): 301-311. <https://doi.org/10.1007/s11030-009-9115-2>.
- Mikulski, D., Eder, K. and Molski, M. (2014). Quantum-chemical study on relationship between structure and antioxidant properties of hepatoprotective compounds occurring in *Cynara Scolymus* and *Silybum Marianum*. *Journal of Theoretical and Computational Chemistry* **13**(1): 1-24. <https://doi.org/10.1142/S0219633614500047>.
- Mitra, I., Saha, A. and Roy, K. (2011). Chemometric QSAR Modeling and In Silico Design of Antioxidant NO Donor Phenols. *Scientia Pharmaceutica* **79**: 31-58. <https://doi.org/10.3797/scipharm.1011-02>.
- Morsy, S.A., Farahat, A.A., Nasr, M.N.A. and Tantawy, A.S. (2017). Synthesis, Molecular Modeling and Anticancer Activity of New Coumarin Containing Compounds. *Saudi Pharmaceutical Journal* **25**(6): 873-883. <https://doi.org/10.1016/j.jsps.2017.02.003>.
- Najafi, M., Mood, K.H., Zahedi, M. Klein, E. (2011). DFT/B3LYP study of the substituent effect on the reaction enthalpies of the individual steps of single electron transfer-proton transfer and sequential proton loss electron transfer mechanisms of chroman derivatives antioxidant action. *Computational & Theoretical Chemistry* **969**: 1-12. <https://doi.org/10.1016/j.comptc.2011.05.006>.
- Nenadis, N. and Tsimidou, M.Z. (2012). Contribution of DFT computed molecular descriptors in the study of radical scavenging activity trend of natural hydroxybenzaldehydes and corresponding acids. *Food Research International* **48**(2): 538-543. <https://doi.org/10.1016/j.foodres.2012.05.014>.
- Ngo, T.C., Dao, D.Q., Thong, N.M. and Nam, P.C. (2016). Insight into the antioxidant properties of nonphenolic terpenoids contained in essential oils extracted from the buds of *Cleistocalyx Operculatus*: A DFT Study. *RSC Advances* **6**(37): 30824-30834. <https://doi.org/10.1039/C6RA02683D>.
- Onar, H.C. and Vardar, B.A. (2018). Synthesis and antioxidant activity of novel 8-formyl-4-substituted coumarins. *Bulletin of the Chemical Society of Ethiopia* **32**(1): 175-178. <https://doi.org/10.4314/bcse.v32i1.17>
- Pe'rez-Cruz, K., Moncada-Basualto, M., Morales-Valenzuela, J., Barriga-González, G., Navarrete-Encina, P., Nuñez-Vergara, L., Squella, J.A. Oleazar, C. (2018). Synthesis and Antioxidant Study of New Polyphenolic Hybrid-Coumarins. *Arabian Journal of Chemistry* **11**(4): 525-537. <https://doi.org/10.1016/j.arabjc.2017.05.007>.
- Rimarcik, J., Lukes, V., Klein, E. and Ilcin, M. (2010). Study of the solvent effect on the enthalpies of homolytic and heterolytic N-H Bond Cleavage in p-phenylenediamine and tetracyano-p-phenylenediamine. *Journal of Molecular Structure: THEOCHEM* **952**(1-3): 25-30. <https://doi.org/10.1016/j.theochem.2010.04.002>.
- Ruscic, B. (2015). Active thermochemical tables: Sequential bond dissociation enthalpies of methane, ethane, and methanol and the related thermochemistry. *The Journal of Physical Chemistry A* **119**(28): 7810-37. <https://doi.org/10.1021/acs.jpca.5b01346>.
- Salem, M.A., Marzouk, M.I. and El-kazak, A.M. (2016). Synthesis and characterization of some new coumarins with in vitro antitumor and antioxidant activity and high protective effects against DNA damage. *Molecules* **21**(2): 249-269. <https://doi.org/10.3390/molecules21020249>.
- Shao, Y., Molnar, L.F., Jung, Y., Kussmann, J., Ochsenfeld, C., Brown, S.T., et al., (2006). Advances in methods and algorithms in modern quantum chemistry program

- package. *Physical Chemistry Chemical Physics* **8**(27): 3172-3191. <https://doi.org/10.1039/B517914A>.
- Shen, Y.F., Liu, L., Feng, C.Z., Hu, Y., Chen, C., Wang, G.X. and Zhu, B. (2018). Synthesis and antiviral activity of a new coumarin derivative against spring viraemia of carp virus. *Fish & Shellfish Immunology* **81**: 57-66. <https://doi.org/10.1016/j.fsi.2018.07.005>.
- Sun, F. and Jin, R. (2013). Theoretical Study on the Radical Scavenging Activity of Shikonin and its Ester Derivatives. *Research Journal of Applied Sciences, Engineering and Technology* **6**(2): 281-284. <https://doi.org/10.19026/rjaset.6.4072>.
- Szeląg, M., Mikulski, D. and Molski, M. (2011). Quantum-chemical investigation of the structure and the antioxidant properties of A-Lipoic acid and its metabolites. *Journal of Molecular Modeling* **18**(7): 2907-2916. <https://doi.org/10.1007/s00894-011-1306-y>.
- Tissandier, M.D., Cowen, K.A., Feng, W.Y., Gundlach, E., Cohen, M.H., Earhart, A.D., Coe, J.V. and Tuttle, T.R.Jr. (1998). The proton's absolute aqueous enthalpy and gibbs free energy of solvation from cluster-ion solvation data. *Journal of Physical Chemistry A* **102**(40): 7787-7794. <https://doi.org/10.1021/jp982638>.
- Wang, G., Xue, Y., An, L., Zheng, Y., Dou, Y., Zhang, L. and Liu, Y. (2015). Theoretical study on the structural and antioxidant properties of some recently synthesised 2,4,5-trimethoxy chalcones. *Food Chemistry* **171**: 89-97. <https://doi.org/10.1016/j.foodchem.2014.08.106>.
- Xia, Y., Chen, C., Liu, Y., Ge, G., Dou, T. and Wang, P. (2018). Synthesis and structure-activity relationship of daphnetin derivatives as potent antioxidant agents. *Molecules* **23**(10): 2476-2489. <https://doi.org/10.3390/molecules23102476>.
- Xie, J. and Schaich, K.M. (2014). Re-evaluation of the 2,2-diphenyl-1-picrylhydrazyl free radical (DPPH) assay for antioxidant activity. *Journal of Agricultural and Food Chemistry* **62**(19): 4251-4260. <https://doi.org/10.1021/jf500180u>.
- Xue, Y., Zheng, Y., An, L., Dou, Y. and Liu, Y. (2014). Density Functional Theory Study of the Structure-Antioxidant Activity of Polyphenolic Deoxybenzoins. *Food Chemistry* **151**: 198-206. <https://doi.org/10.1016/j.foodchem.2013.11.064>.
- Yap, C.W. (2011). PaDEL-descriptor: An open source software to calculate molecular descriptors and fingerprints. *Journal of Computational Chemistry* **32**(7): 1466-1474. <https://doi.org/10.1002/jcc.21707>. Epub 2010 Dec 17.
- Zheng, Y.Z., Deng, G., Liang, Q., Chen, D.F., Guo, R. and Lai, R.C. (2017). Antioxidant activity of Quercetin and its glucosides from Propolis: A theoretical study. *Scientific Reports* **7**(1): 7543-7554. <https://doi.org/10.1038/s41598-017-08024-8>.
-